TGFα, c-MYC, mutated CTNNB1 and their combinations act distinctly on the Hep3B tumors in nude mice

TGFα, c-MYC, mutated CTNNB1 and their combinations act distinctly on the Hep3B tumors in nude mice.

Hidenao Noritake[1,2], Mohammed Badrul Amin[1], Kasumi Nakamura[1,3], Mohammod Johirul Islam[1], Yi-Xin Wu[1], Satoru Hashimoto[1], Mohammad Khaja Mafij Uddin[1], Takafumi Suda[2], Yoshimasa Kobayashi[2], Haruhiko Sugimura[4], Naoyuki Miura[1,*]

Departments of [1]Biochemistry, [2]Internal Medicine, [3]Oral and Maxillofacial Surgery and [4]Tumor Pathology, Hamamatsu University School of Medicine, 1-20-1 Handa-yama, Higashi-ku, Hamamatsu 431-3192, Japan

(Received ; Accepted)

ABSTRACT

Hepatocellular carcinoma (HCC) is the most common hepatic tumor worldwide and is a major cause of death in many countries. Although chronic viral infections and hepatotoxic agents are the major risk factors, the molecular pathogenesis of HCC remains largely unknown. Among model mice, *TGFα/c-Myc* transgenic mice develop human HCC-like tumors. Whole genome sequencing of HCC tumors from patients has shown that mutations to *CTNNB1* (β-catenin) are the most frequent (15.9%). So in this study, we characterized the effects of *TGFα*, *c-MYC* and *mutant CTNNB1* genes on the transplantable Hep3B cells. *TGFα* increased the tumor number after transplanting Hep3B cells. *Mutant CTNNB1* changed the characteristics of Hep3B tumor cells into a disarranged structure with loose cell-cell contacts. And co-transduction of *TGFα* and *mutant CTNNB1* synergistically increased the growth rate, size and weight of Hep3B tumors. Unexpectedly, *c-MYC* overexpression in the Hep3B cells induced apoptosis. Interestingly, *TGFα+mutant CTNNB1+MYC*-transduced cells grew very slowly and the tumor showed transdifferentiation into a cholangial duct. These results suggest that the interaction of these three genes determines the characteristics of Hep3B tumor. Overexpression of *c-MYC* by a lentivirus in *c-MYC*-upregulated HCC tumors might be used as a molecular targeted therapy.

Key Words: TGFα, C-MYC, mutant CTNNB1, HCC, apoptosis, transdifferentiation

INTRODUCTION

Hepatocellular carcinoma (HCC) is the most common primary hepatic malignancy. Its incidence and prevalence is globally heterogeneous with the highest rates in southeast asia and sub-Saharan Africa. In Western industrialized nations, its incidence has significantly increased in the past three decades. Its global heterogeneity is, in part, a reflection of the global distribution of its risk factors. Its prognosis is dismal with a five-year survival of 11%. The only potentially curative treatment is surgical with either resection or orthotopic liver transplantation. However, the majority of HCC patients are diagnosed at an advanced stage at which surgical therapies are not feasible (1).

The causative genes in HCC are not known. The most frequent etiology is the patients with chronic infection with hepatitis C virus or B virus. Investigations have been performed to discover mutations in HCC. In a small number of patients with HCC, the mutation of β-catenin (*CTNNB1*) was found next to *TP53* (2). In order to find the causative genes for HCC, many genetically modified mice have been produced. Among them, only the transgenic mice that produce TGFα and c-Myc shows HCC-like tumors (3-5). The transgenic mouse harboring the *mutated CTNNB1* gene does not show tumorgenesis but does exhibit a more rapid onset of chemical carcinogenesis (6). We focused oncogenes, but not anti-oncogenes. Therefore we aimed to evaluate the effects of *TGFα*, *c-MYC* and *mutated CTNNB1*, the most possible HCC inducers, on the tumor formation in Hep3B cells. We found that *TGFα* tended to increase the transplantability in Hep3B cells in nude mice, *c-MYC* antagonized the action of TGFα by inducing apoptosis and *mutated CTNNB1*worked cooperatively with *TGFα* to increase the growth of tumors.

MATERIALS AND METHODS

Cell culture

Hep3B, HepG2, Huh6.5 and Huh7.5 cells were cultured in Dulbecco's modified Eagle Medium (DMEM) supplemented with 10% fetal calf serum (FCS).

Lentivirus production

Human total RNA was purchased from Ambion (Naugatack, CT, USA). cDNA was made from this RNA with Primescript (Takara, Kyoto, Japan). TGFα cDNA were obtained by polymerase chain reaction (PCR) with the following primers using Phusion (New England Biolab, MA); 5'-ATGGTCCCCTCGGC TGGCA-3' and 5'-CTGGGCTCTTCAGACCACT G-3'.

Human c-MYC and CTNNB1 cDNAs were purchased from Origene Technologie (MD, USA). The in vitro mutagenesis of ^{33}Ser/^{37}Ser/^{41}Thr/^{45}Ser of CTNNB1(β-catenin) into four Ala residues was performed by PCR with the mutant oligonucleotide, 5'-CAGTCTTACCTGGACGCTGGAATCCATGCTG GTGCCACTGCCACAGCTCCTGCTCTGAGTGGT AAAGG-3'. Mutated CTNNB1, designated CTNNB1(4A), was confirmed by sequening. The enhanced activity of CTNNB1(4A) was demonstrated by transfecting wild-type CTNNB1 and CTNNB1(4A) cDNAs with TOP and FOP reporter plasmid DNAs into 293T cells (7, 8).

A lentivirus was produced by transfecting CSII-EF-MCS-IRES2-Venus (containing a cDNA), pCAG-HIVgp and pCMV-VSV-G-RSV-Rev plasmid DNAs into 293T cells by the protocol established by Dr. H. Miyoshi. These plasmid DNAs were provided by Dr. H. Miyoshi, Bioresource Research Center, DNA Bank, RIKEN (Tsukuba, Japan). The TGFα, MYC and CTNNB1(4A) cDNAs were inserted into the BamHI or Not I site of the CSII-EF-MCS-IRES2-Venus plasmid DNA to make CS-EF-TGFα, CS-EF-MYC and CS-EF-CTNNB1(4A) DNAs, respectively.

Infection of lentivirus into Hep3B cells and transplantation of infected Hep3B cells into nude mice.

Hep3B cells were plated at a density of $1x10^5$ cells/mL in 6-well plates and cultured at 37°C in a humidified 5% CO_2 atmosphere in DMEM with 10% FCS. Twenty-four hours later the medium was aspirated and cells were washed by PBS (phosphate-buffered saline), and new DMEM containing the lentiviral vectors were added to each plate and incubated for another 48 h. Flow cytometric analysis was performed with a FACS Aria flow cytometer (Becton Dickinson Systems, San Jose, CA) and Venus-positive Hep3B cells were collected. Then these cells were plated again and cultured as described above.

Infected Hep3B cells ($1x10^6$ cells in 0.25mL DMEM) were injected subcutaneously using a 26-gauge needles into the right and left flank of 8- to 10-week old BALB/c nu/nu mice (SLC Inc., Shizuoka, Japan). These mice were housed in a laminar flow caging system and all food, bedding, and water were autoclaved. The longest dimension of each tumor was measured every week. After eight weeks, mice were sacrificed and the tumors were enucleated and weighed.

Immunohistochemical analysis of tumor formation in the transplanted tissues

Each tumor was fixed in 10% neutral-buffered formalin for 48 h, processed routinely, and stained with hematoxylin and eosin (HE). The tumors for immunohistochemical examination were fixed with 10% neutral-buffered formalin, embedded in paraffin, and the sections were cut at 5 μm. The sections were deparaffinized in xylene, and hydrated through a graded series of ethyl alcohols, and washed. Endogenous peroxidase activity in the sections was inhibited by treating with 3% H_2O_2 for 5 minutes, and then the sections were rinsed. A tissue microarray containing representative xenografts (4mm in diameter) from each group was prepared according to a previously published method (9, 10).

Antibodies against the following human proteins were used to characterize the xenografts introduced by each combination of genes: prealbumin (GeneTex Inc., Irvine, CA, USA), CYP3A4 (Bioss Inc. Boston, MA, USA), β-catenin (Leica Biosystems, Buffalo Grove, IL), sFRP1 (Novus Biologicals, Littleton, CO, USA), α-fetoprotein (AFP, DAKO, Copenhagen, Denmark), connexin 32 (Novus Biologicals), CK19 (DAKO), TP53 (DAKO), LIX1L (Abnova, Heidelberg, Germany), CD44v (a gift from Prof Hideyuki Saya, Keio University, Tokyo)(11), SALL4 (Abnova), E-cadherin (NOVOCASTRA, New Castle upon Tyne, UK), CDX2 (BioCARE, Lujhu Township, Taiwan), hepatocyte (Clone OCH1E5, DAKO), and MET

(Abcam). Monoclonal mouse anti-DPP-4 and anti-serpin antibodies were made in our laboratory (Hayashi Y, Miura N, manuscript in preparation). Visualization was performed using secondary antibodies conjugated with peroxidase.

Isolation of total RNA from the Hep3B cells and reverse transcriptase-polymerase chain reaction (RT-PCR)

Cultured Hep3B cells were washed with PBS and lysed in 5.5 M guanidine thiocyanate (Sigma), 25 mM sodium citrate, 0.5% Sarkosyl and 0.2 M β-mercaptoethanol. After DNA cleavage, the solution was applied onto 5 mL of 5.7 M CsCl in a SW41 tube and centrifuged at 27,500 rpm at room temperature for 12 h. The pellet (RNA) was washed with 70% ethanol and dissolved in H_2O. Human liver RNA was purchased from Ambion.

Five micrograms of total RNAs from human liver and Hep3B cells were reverse-transcribed with PrimeStar (Takara, Kyoto), boiled for 5 min and the diluted with four volumes of H_2O. PCR was performed with the following primers. 5-GAGGC GTAGGAATGAGGCTG-3' and 5'-CAG GGAGCTT GCAGAGATGG-3' for TGFα, 5'-TCCTCACA GCCCACTGGTCC-3' and 5'-GCTCCTCTGCTTG GACGGAC-3' for c-MYC, 5'-TGCCCAGGGA GAA CCCCTTG-3' and 5'-CCACTCCCACCCTACCAA CC-3' for CTNNB1 (β-catenin) and 5'-CTGGAG CTGGCAAGGTCACC-3' and 5'-GTCTCGGTGTT GACCAAAGG-3' for EF1A1. PCR products were separated on a 6% polyacrylamide gel.

Apoptosis assay

Lenctivirus-infected cells were subjected to FACS and Venus-positive cells were collected, plated and cultured as described above. In one day after absorbing the activation light, about half of the cells were dead. Apoptotic cells were detected by cell morphology and by Annexin V staining (Biovision, Milpitas, CA, USA)

RESULTS

As a preliminary experiment, we transplanted four available hepatoma cell lines, Huh7.5, HepG2, Hep3B and Huh6.5. After eight weeks, we prepared HE-stained sections from the tumors in nude mice (Fig. 1). Huh7.5 and Hep3B tumors exhibited a thick trabecular pattern consistent with the typical picture of human hepatocellular carcinoma (Fig. 1A, 1B), while the HepG2-derived tumor had blastic features consistent with its origin of hepatoblastoma (Fig.1C). Huh6.5 tumors showed a duct forming feature (Fig. 1D). Although all of these tumors showed morphological characteristics of malignancy, Hep3B cells seemed to be rather differentiated than Huh7.5 cells, so we chose Hep3B cells as a the target of transfection with the following combinations of multiple genes. We constructed lentiviruses expressing *TGFα, c-MYC* and *CTNNB(4A)*.

Before infection by lentiviruses, we measured the baseline expression of *TGFα, c-MYC* and *CTNNB1* mRNA in cultured Hep3B cells by RT-PCR method (Fig.2). These three mRNAs were up-regulated in Hep3B cells compared to normal human liver cells.

In our lentivirus constructs, Venus protein was used as a monitor of expression of the upstream gene (*TGFα, c-MYC* or *CTNNB(4A)*) inserted because the Venus gene was connected the upstream gene via an IRES. Forty-eight hours after infection, we collected Venus-positive Hep3B cells using a cell sorter and cultured them for two weeks. Unexpectedly, the *MYC-, MYC+TGFα-* and *MYC+CTNNB(4A)*-transduced Hep3B cells died during two-week culture period. Transduction of *TGFα+MYC+CTBNNB(4A)* into Hep3B cells made them grow at a slower rate than when the other combinations of genes were transduced. Then we transplanted 10^6 cells of the control (parental Hep3B) and four transduced cell lines, i.e. Hep3B cells that were transduced by four combinations of genes, into the flank of nude mice (10 points per group). We measured the diameter of the tumors every week for eight weeks, at which point the tumors were taken out and subjected to HE staining and immunohistochemical examination. Unfortunately, two mice died due to unknown reasons.

The number of tumors in each group is summarized in Table 1. Transduced overexpression of *TGFα* tended to increase the number of tumors while overexpression of stable β-catenin (the product of *CTNNB(4A)*) decreased the number of tumors. The time course of tumor size in each group is shown in Fig. 3. The *TGFα*-overexpressing Hep3B tumors grew at a similar rate compared to the control Hep3B tumors. The *TGFα+CTNNB(4A)*- overexpressed Hep3B tumor grew faster than control. *CTNNB(4A)*- and *TGFα+CTNNB(4A)+MYC*-transduced Hep3B tumors grew more slowly than the control.

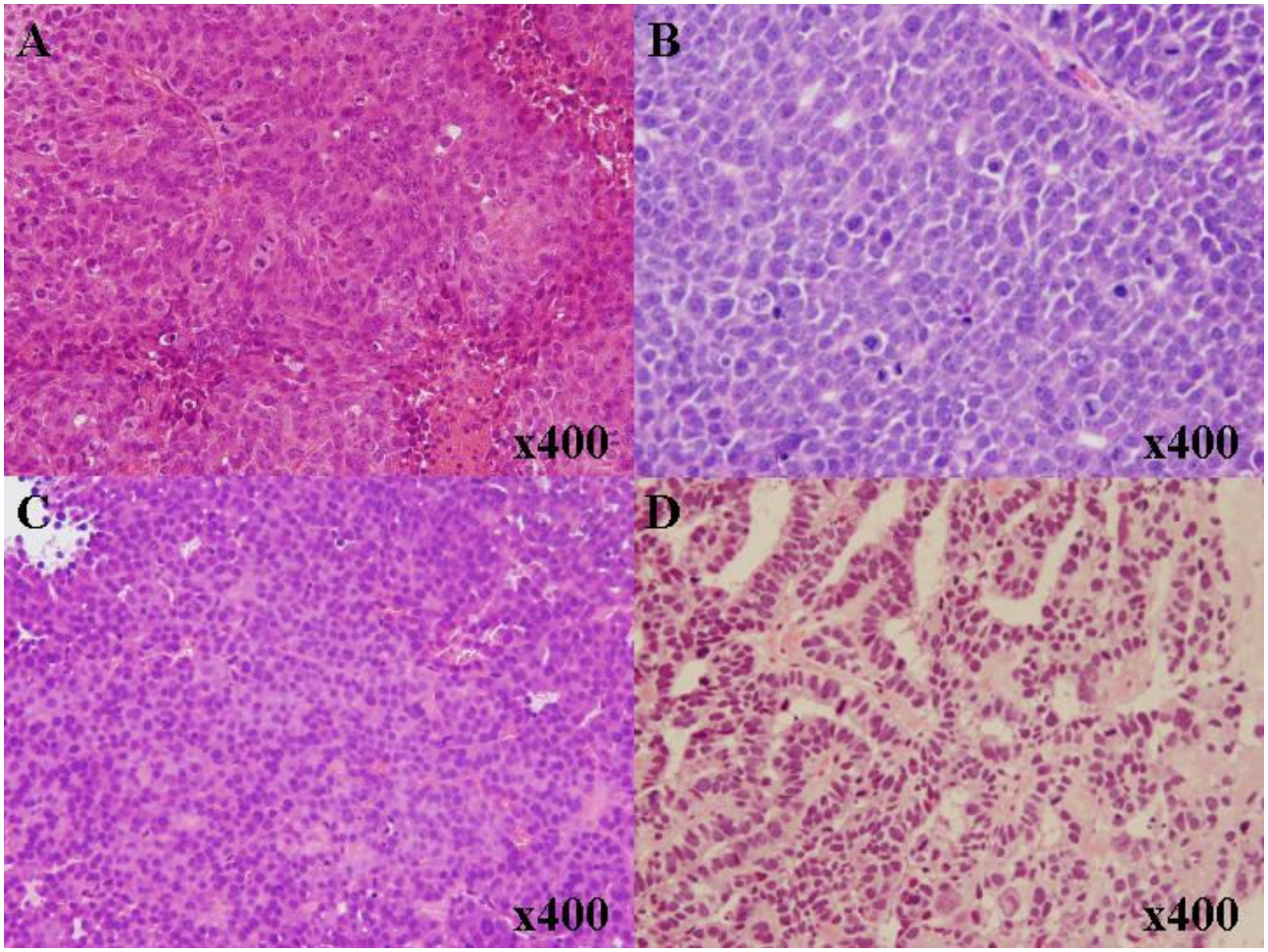

Fig. 1 HE staining of tumors transplanted with Huh7.5, Hep3B, HepG2 and Huh6.5 cells. Four kinds of hepatoma cells (1 X 10^6 cells) were injected into the subcutaneous tissues on the back of nude mice. After eight weeks, the tumors were excised, fixed and stained with hematoxylin and eosin. A, Huh 7.5 cells; B, Hep3B cells; C, HepG2 cells; D, Huh6.5 cells.

Table 1. Effect of oncogenes on the transplantability of Hep3B cells

Oncogenes	Number of tumors/transplanted sites
Control	3/10
TGFα	5/8
TGFα+CTNNB1(4A)	2/8
TGFα+CTNNB1(4A)+MYC	1/10
CTNNB1(4A)	1/10
CTNNB1(4A)+MYC	Unable
TGFα+MYC	Unable
MYC	Unable

Unable; Infected Hep3B cells were dead before transplantation.
Control vs. TGFα; P=0.184
TGFα vs. TGFα+CTNNB1; P=0.157
TGFα vs. TGFα+CTNNB1+MYC; P=0.032
TGFα vs. CTNNB1; P=0.032

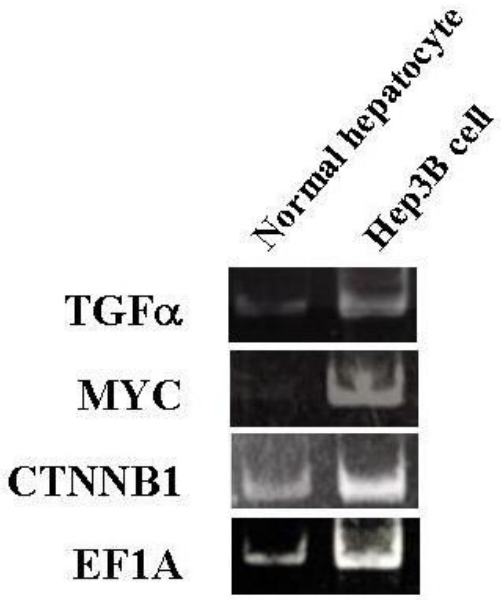

Fig.2 *TGFα*, *MYC* and *CTNNB1* in the human liver and Hep3B cells. Five μg of RNA from human liver and Hep3B cells were reverse-transcribed and the cDNAs were used as a template for PCR. EF1A1 was used as the control.

After eight weeks, the tumors were taken out and the diameter and weight of tumors were measured (Figs. 4 and 5). *TGFα+CTNNB(4A)* significantly increased the diameter and tended to increase the weight of tumors compared to control and *TGFα*-transduced Hep3B tumors. Although only one *TGFα+CTNNB1(4A)+MYC*-transduced tumor was found, *c-MYC* decreased the increasing weight by the *TGFα+CTNNB(4A)* synergistic action in the *TGFα+CTNNB(4A)+MYC* tumor (Fig. 5).

Next we examined HE staining of tumors in each group (Fig.6). The subcutaneous tumors derived from parental Hep3B cells showed ill-defined trabecular patterns and polygonal cancer cells had round nuclei with fine chromatin and prominent nucleoli (basophilic clear nuclei). Cell division was observed in 3-4% of these tumor cells (Fig. 6A). The *TGFα*-transduced tumors showed small and large pale nuclei in most of the population. Notably, these tumors occasionally had very large cells with large nuclei (Fig. 6B, arrowheads). *CTNNB1(4A)*- transduced Hep3B tumors showed disorganized cell arrangements and loose cell-cell contacts and some heterogeneous populations were identified (Fig. 6C).

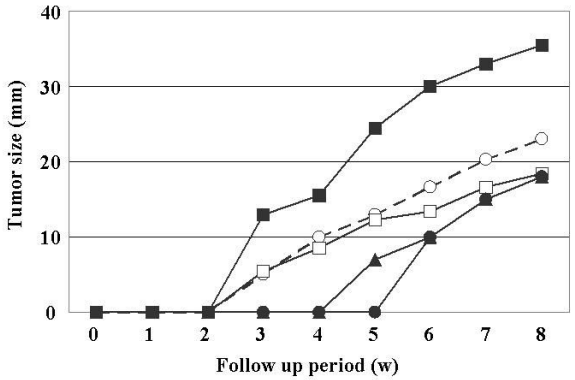

Fig. 3 Time course of the diameter of the tumors infected with various lentiviruses. ○,Control; □, TGFα; ●, CTNNB1(4A); ■, TGFα+CTNNB1(4A); ▲, TGFα+CTNNB1(4A)+MYC.

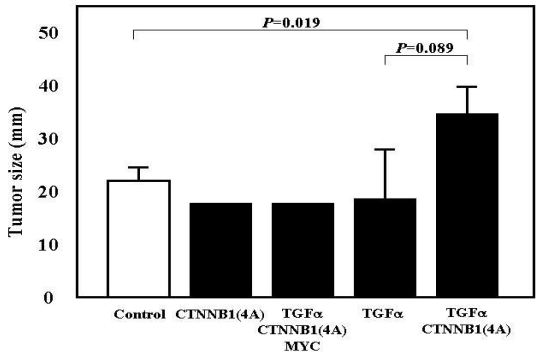

Fig. 4 Comparison of the diameter of tumors infected with various lentiviruses

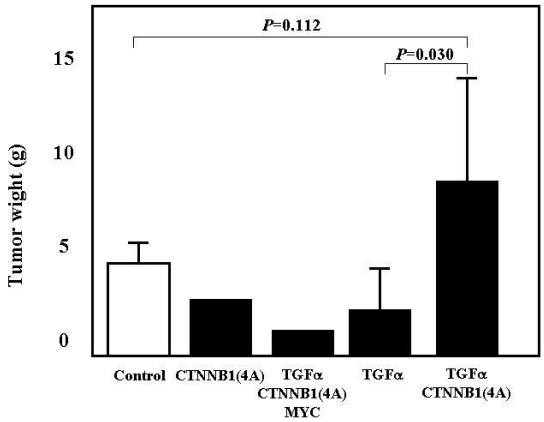

Fig. 5 Comparison of the weight of tumors infected with various lentiviruses

TGFα+CTNNB1(4A)-overexpressing Hep3B cells showed similar characteristics to *TGFα*-transduced cells (Fig. 6D,6B), but mitotic figures were more prominent. Interestingly, additional *TGFα* transduction reversed the disarrangements and cell-cell contact defects seen in the *CTNNB1(4A)*-transduced tumors (compare Fig. 6D to 6C). *TGFα+CTNNB1(4A)+MYC*-transduced tumors showed a duct-like structure in some parts, although the polarity of the lining cells was vague (Fig. 6E,6F).

Next, we immunostained tumors with 17 antibodies to characterize and estimate the morphological effects of transduced genes. Membranous staining of β-catenin was shown in parental Hep3B cells and in *TGFα*-transduced tumors (Fig. 7A, 7B). In *CTNNB1(4A)*-transduced tumors, cell membrane staining was stronger and a considerable portion of tumors cells exhibited nuclear staining (Fig. 7C). In contrast, the most of the *TGFα+CTNNB1(4A)*-transduced tumors showed only membrane staining of β-catenin, and nuclear localization of β-catenin was rarely seen (Fig. 7D). In *TGFα+CTNNB1(4A)+MYC*-transduced tumors, strong membranous staining was seen in the ductal regions and in other parts (Fig. 7E). Next, immunostaining for CD44v, a cancer stem cell marker (11), showed similar pattern in all tumors (Fig. 7F-7J). MET, a receptor for hepatocyte growth factor, was diffusely and weakly positive in the membrane of the cells in all the xenografts (Fig. 7K-7O).

We immunostained tumors with the antibodies against diffrentiation markers, i.e. cytokeratin 19 (CK19) as a bile duct marker, hepatocyte (Hep) as a hepatocyte marker. In the immunostaining with the CK19 antibody (Fig. 8A-8E), all tumors were negative, except for the ductal structures brought about by the transduction of all three genes, which were positive (Fig. 8E). Hepatocyte antibody immunoreactivitiy was expected to be positive in the cells of hepatocytic differentiation. The ductal portion in *TGFα+CTNNB1(4A)+MYC*-transduced cells was negative (Fig. 8J). Furthermore, some undifferentiated cells in the *TGFα−* and *TGFα+CTNNB1(4A)*-transduced xenografts were also negative for the anti-Hep antibody (Fig. 8F-8J). LIX1L, a newly identified marker for the bile duct epithelium (Fig. 8K-8O, Satoki Nakamura, personal communication), was also positive only in the ductal structure in the cells transduced by all three genes (Fig. 8O).

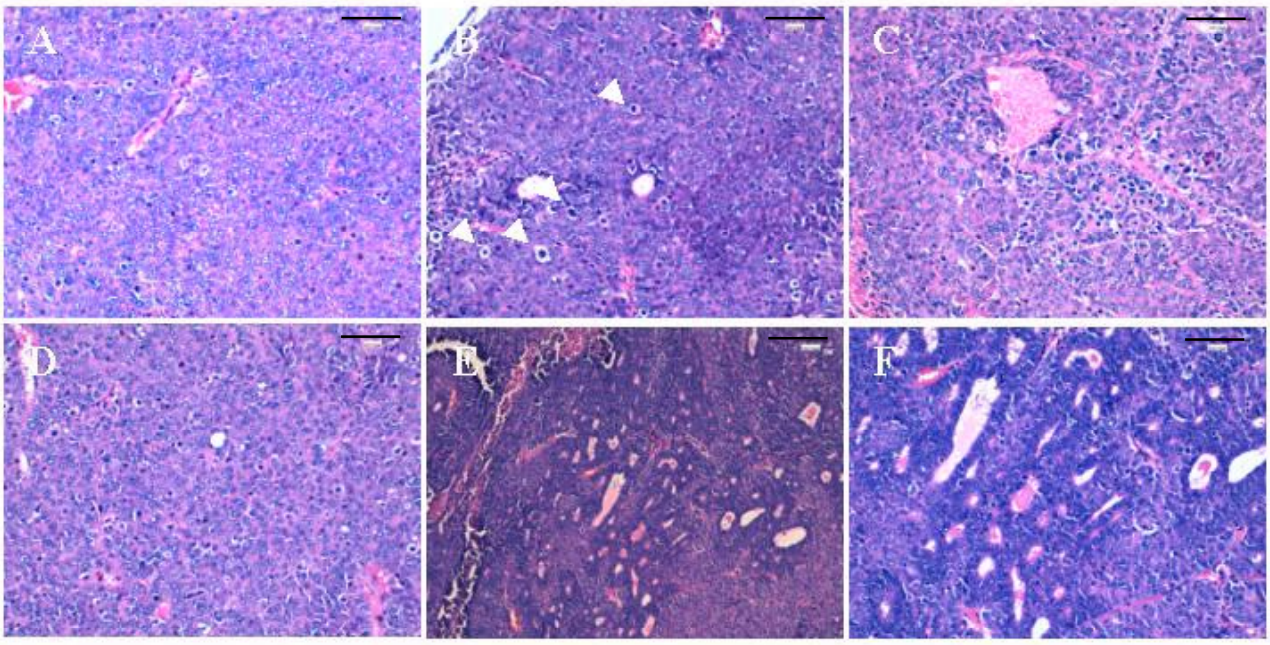

Fig. 6 HE staining of tumors infected with various lentiviruses. A, Control tumors with no transduced Hep3B cells. B, Tumor transplanted with the *TGFα*-transduced Hep3B cells. C, Tumor transplanted with *CTNNB(4A)*-transduced Hep3B cells. D, Tumor transplanted with *TGFα+CTNNB(4A)*-transduced Hep3B cells. E, Tumor transplanted with the *TGFα+CTNNB(4A)+MYC*-transduced Hep3B cells. F, Ductal structure, magnified picture of E. Bars, 100 μm

Immunostaining with other antibodies, such as anti-prealbumin, anti-CYP3A4, anti-AFP, anti-CDH1, and anti-connexin 32 antibodies were diffusely positive and did not show any differences among the groups of tumors (data not shown). Stainings with antibodies against P53, sFRP1, SALL4 and CDX2 was completely negative in nuclei (data not shown). Serpin and DPP4 immunostaining was diffusely positive in the membrane of the cells, but differences among the groups were not found (data not shown).

Finally, we observed that overexpression of *c-MYC* induced apoptosis in *Myc-*, *MYC+TGFα-* and *MYC+CTNNB1(4A)*-transduced Hep3B cells. Therefore, we collected the Venus-positive cells after *MYC, TGFα, CTNNB1(4A), TGFα+MYC* and *MYC +CTNNB1(4A)* lentiviral infection and cultured the transduced cells. The *TGFα-* and *CTNNB1(4A)*-ransduced Hep3B cells grew at similarly to control Hep3B cells on days 1 and 5. However, the *MYC*-transduced Hep3B cells showed apoptosis on day 5. Furthermore, *MYC+TGFα-* and *MYC+ CTNNB1(4A)*-transduced Hep3B cells showed evidence of apoptosis on days 1 and 5 (Fig. 9). From this result, we interpret that the synergistic action of *TGFα* and *CTNNB1(4A)* might overcome the apoptotic action of *c-MYC* in *TGFα+CTNNB1(4A)+ MYC*-transduced cells.

DISCUSSION

We examined the effects of the overexpression of probable HCC inducer genes, i.e. *TGFα, c-MYC* and *mutated CTNNB1 (CTNNB1(4A))*, on the characteristics of transplanted tumors when these genes were transduced into Hep3B cells. *TGFα* increased the tumor number in nude mice, although this was not statistically significant. Clearly, *CTNNB1(4A)* inhibited the effects of *TGFα* effect in terms of increased tumor number in *TGFα+ CTNNB1(4A)* tumor (Table 1). TGFα might increase the number of tumors by a paracrine action while mutant β-catenin might increase a cell density, not the number. However, the synergistic action of *TGFα+ CTNNB1(4A)* increased the growth rate, size and weight of tumors compared to *TGFα-* or *CTNNB1(4A)*-transduced tumors (Figs. 3, 4 and 5). In contrast, *CTNNB1(4A)* alone and *TGFα+ CTNNB1(4A)+MYC* decreased the growth rate and size of tumors compared to control.

In the morphological comparisons, control tumor cells displayed homogenous-sized cells with homogenous basophilic clear nuclei. *TGFα*-transduced Hep3B tumors were heterogenous in character: cell nuclei were variable in size, and ranged from basophilic clear to eosinophilic dark. In contrast, the *CTNNB1(4A)*-transduced Hep3B tumors showed a disarranged structure and loosecell-cell contact. Unexpectedlly, a ductal character was seen in the *TGFα+CTNNB1(4A)+MYC*-transduced tumors (Fig.6).

In the immunohistochemical analysis of β-catenin, many *CTNNB1(4A)*-transduced tumor cells showed nuclear localization of mutant β-catenin, which is associated with cell proliferation. Interestingly, in the *CTNNB1(4A)+TGFα*-transduced tumor cells, mutant β-catenin was localized not in the nucleus, but mainly in the membranes with some in the cytoplasm. This phenomenon has been reported previously in the c-Myc and c-Myc/TGFα transgenic mice. In that experiment, the mutations of β-catenin occurred in both mice: 23.5% of the c-Myc transgenic background showed nuclear localization of mutant β-catenin, but none of the c-Myc/TGFα transgenic mice showed nuclear localization (12). Taken together with our data, it is likely that TGFα may interfere with the transfer of mutant β-catenin into the nucleus. For example, it may affect the stable interaction of mutant β-catenin with Axin, Apc and Conductin in the cytoplasm, enhance the binding of mutant β-catenin with E-cadherin, α-catenin, p120 and 14-3-3 under the membrane, or inhibit the binding of the protein that transfers mutant β-catenin to the nucleus. This issue should be resolved in the near future.

Overexpression of c-MYC in the *MYC-,MYC+ TGFα* and *MYC+CTNNB(4A)*-transduced cells resulted in apoptotic death, as shown in Fig.9. *c-MYC* was already upregulated in Hep3B cells (Fig. 2). Further overexpression of c-MYC in the parental and *TGFα-* or *CTNNB1(4A)*-transduced Hep3B cells may have exceeded a safety level and promote cell death.

MYC-induced apoptosis has been reported previously (13, 14). In the case of *TGFα+ CTNNB1(4A)+MYC*-transduced Hep3B cells, the survival stimulus (*TGFα+CTNNB1(4A)*) may have been stronger than the death stimulus (*c-MYC*). However, as a result, proliferation was inhibited and was so slow that a different cell character was induced, that is, transformation into a cholangial duct. This concept is supported by the CK19-positive, Hep-negative and LIX1L-positive duct structure (Fig. 8E, 8J, 8O). The unique status of TGFα, c-MYC and mutant β-catenin may shift the cell fate from hepatocyte into bile duct.

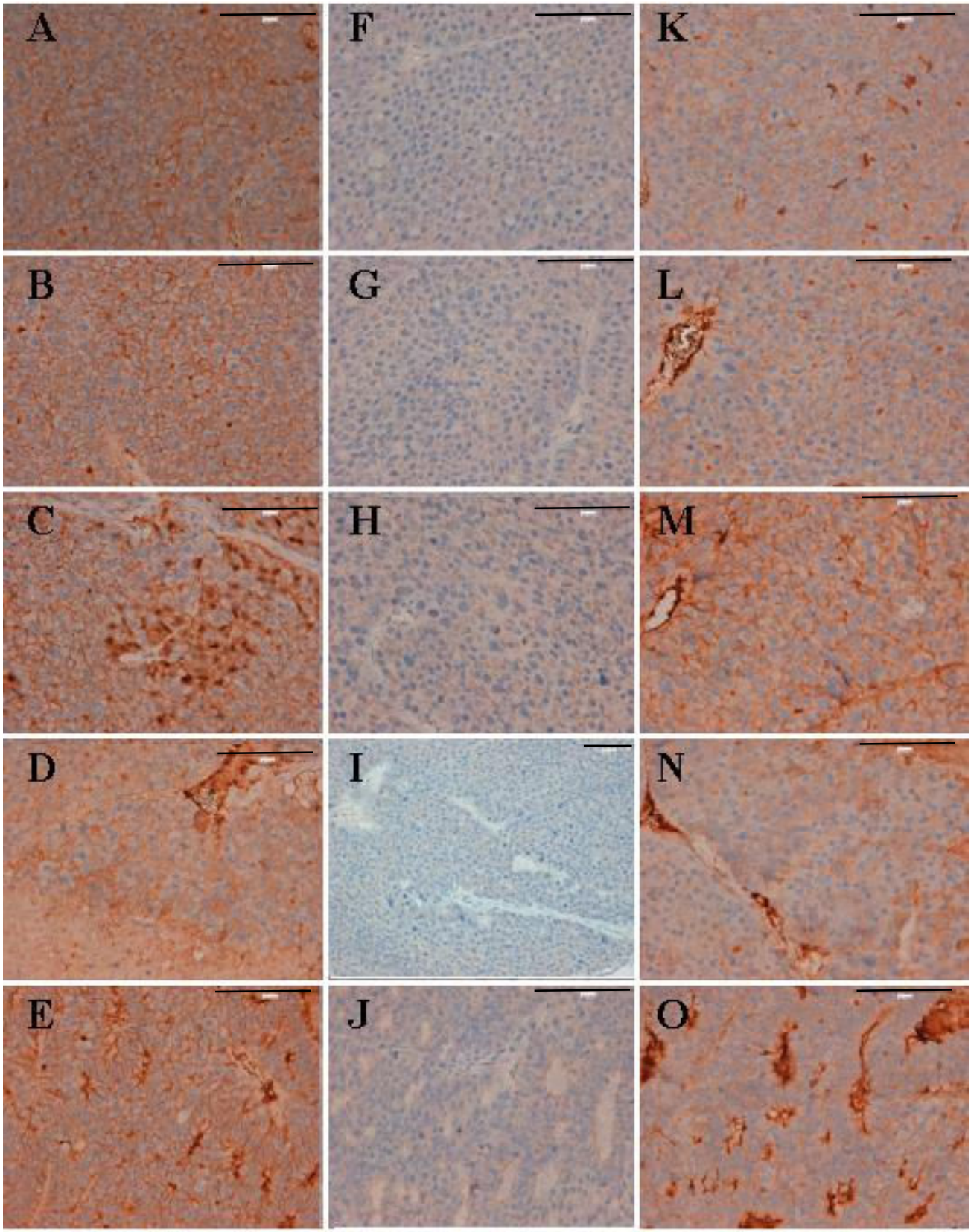

Fig. 7 Immunostaining for β-catenin, CD44v and MET in the tumors. Control tumors with non-transduced Hep3B cells (A,F,K), tumor transplanted with the *TGFα*-transduced Hep3B cells (B,G,L), tumor transplanted with *CTNNB(4A)*- transduced Hep3B cells (C,H,M), tumors transplanted with *TGFα+CTNNB(4A)*-transduced Hep3B cells (D,I,N), and tumor transplanted with the *TGFa+ CTNNB(4A)+MYC*-transduced Hep3B cells (E,J,O). Tumors were immunostained with anti-β-catenin antibody (A-E), anti-CD44v antibody (F-J) and anti-MET antibody (K-O). Note that the nuclear localization of mutant β-catenin is shown in C and nuclear localization is lost in D and E. Bars, 100 μm.

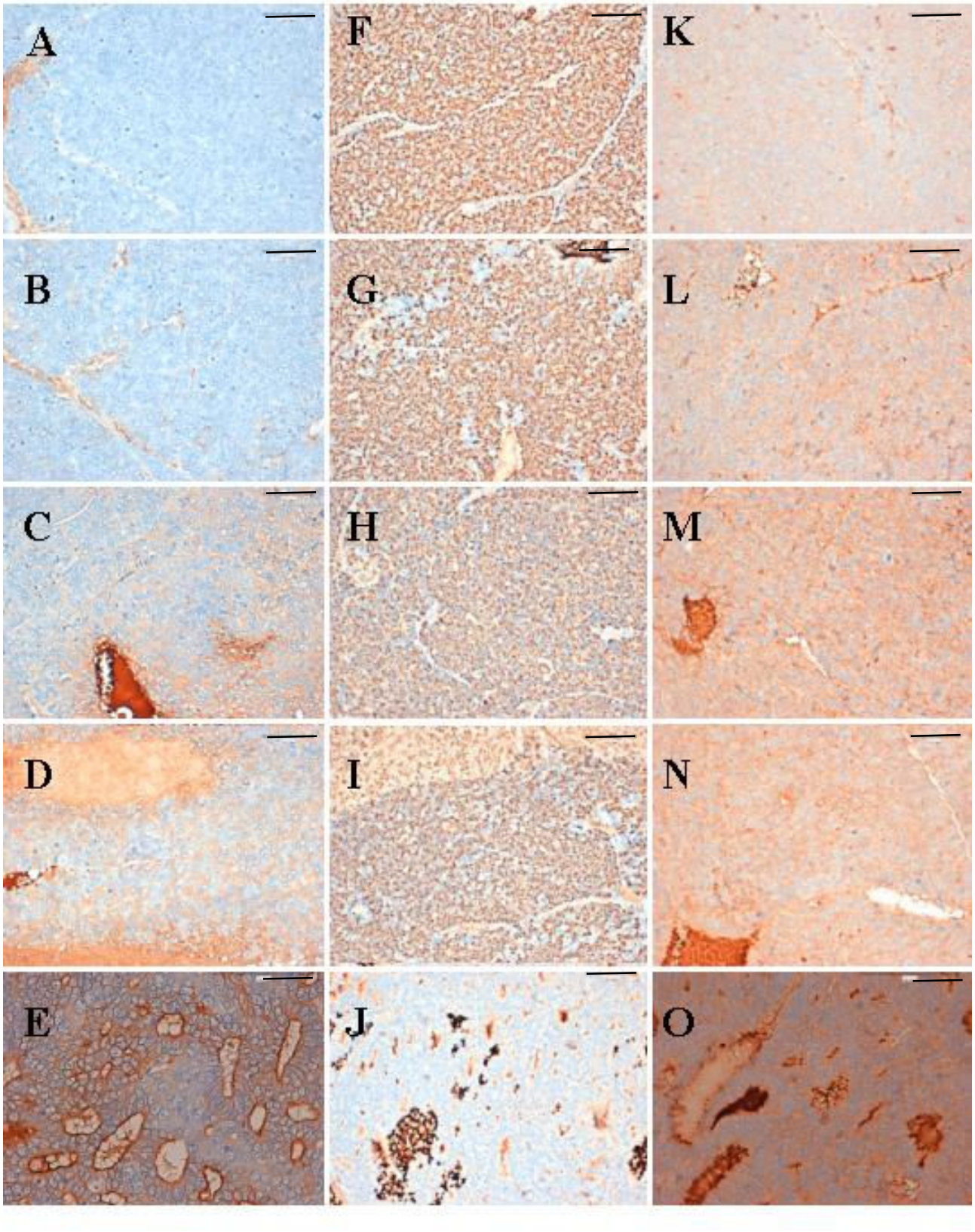

Fig. 8 Immunostaining for CK19, Hep and LIX1L in the tumors. Control tumors with non-transduced Hep3B cells (A,F,K), tumor transplanted with the *TGFα*-transduced Hep3B cells (B,G,L), tumor transplanted with *CTNNB1(4A)*-transduced Hep3B cells (C,H,M), tumors transplanted with *TGFα+CTNNB(4A)*-transduced Hep3B cells (D,I,N), and tumor transplanted with the *TGFa+CTNNB(4A)+MYC*-transduced Hep3B cells (E,J,O). Tumors were immunostained with anti-cytokeratin 19 (CK19)(A-E), anti-hepatocyte (Hep)(F-J) and anti-LIX1L (K-O) antibodies. Bars, 100 μm.

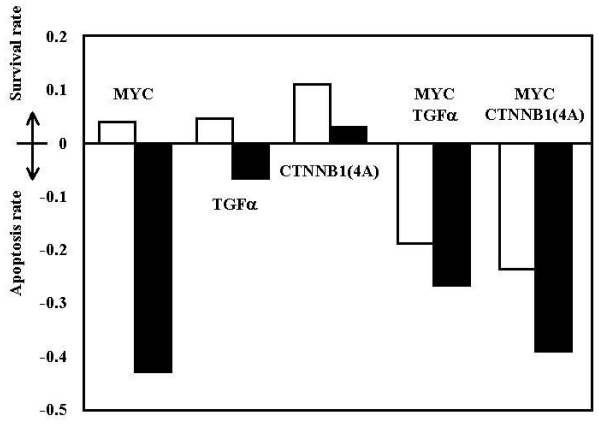

Fig. 9 c-Myc induced apoptosis in the overexpressing Hep3B cells. Infected Hep3B cells were collected using a cell sorter. Venus-positive Hep3B cells were plated in 24 well plates. After 1 (open bars) and 5 (closed bars) days, the apoptosis rate (the numbers of apoptotic cells is divided by the numbers of live cells plus apoptotic cells) was calculated and the value of control Hep3B cells was used as zero after 1 and 5 days. Plus indicates the survival rate and minus indicates the apoptosis rate (Range; +0.54~-0.46 after 1 day and +0.29~-0.71 after 5 days). Note that *TGFα* and *CTNNB1(4A)* did not affect the survival/apoptosis rates compared to the parental Hep3B cells prominently while *c-MYC* induced apoptosis in the *Myc-, MYC+TGFα* and *MYC+CTNNB1(4A)*- transduced Hep3B cells.

ACKNOWLEDGMENTS

We acknowledge Hisaki Igarashi for performing HE and immunohistochemical staining. This work was supported by a Grant-in-Aid from the Ministry of Education, Science, Sports, Culture and Technology of Japan [23659645, 24659603], a Grant-in-Aid from the U.S.-Japan Cooperative Medical Science Program; the National Cancer Center Research and Development Fund (25A-1), a grant for priority areas from the Japanese Ministry of Education, Culture, Sports, Science and Technology [221S0001], Grants-in-Aid for Cancer Research from the Japanese Ministry of Health, Labor and Welfare [23120201 and 10103838], the Smoking Research Foundation, and the Princess Takamatsu Cancer Research Fund.

REFFERENCES

1. Blechacz B, Mishra L. Hepatocellular Biology. In *Multidisciplinary treatment of hepatocellular carcinoma*, Recent Results in Cancer Research (Vauthey J-N, Brouquet A (eds.)) Springer Verlag, Berlin Heiderberg, 2013: 1-20
2. Kan Z, Zheng H, Liu X, Li S, Barber TD, Gong Z, Gao H, Hao K, Willard MD, Xu J, Hauptschein R, Rejto PA, Fernandez J, Wang G, Zhang Q, Wang B, Chen R, Wang J., Lee NP, Zhou W, Lin Z, Peng Z, Yi K, Chen S, Li L, Fan X, Yang J, Ye R, Ju J, Liu J, Ehsani ME, Zhang C, Loboda A, Sung WK, Aggarwal A, Poon RT, Fan ST, Wang J, Hardwick J, Reinhard C, Dai H, Li Y, Luk JM, Mao M. Whole-genome sequencing identifies recurrent mutations in hepatocellular carcinoma. Genome Res 23: 1422-1433. 2013.
3. Murakami H, Sanderson ND, Nagy P, Marino PA, Merlino G, Thorgeirsson. Transgenic mouse model for synergic effects of nuclear oncogenes and growth factors in tumorigenesis: interaction of c-myc and trans forming growth factor a in hepatic oncogenesis. Cencer Res 53: 1719-1723. 1993.
4. Lee J-S, Chu I-S, Mikaelyan A, Calvisi DF, Heo J, Reddy JK, Thorgeirsson. Application of comparative functional genomics to identify best-fit mouse models t study human cancer. Nat Genet 12: 1306-1311. 2004.
5. Calvisi DF, Factor VM, Ladu S, Conner EA, Thorgeirsson SS. Disruption of β-catenin pathway or genomic instability define two distinct categories of liver cancer in transgenic mice. Gastroenterology 126: 1374-1386. 2004.
6. Ichihara T, Komagata Y, Yang X-L, Uezato T, Enomoto K, Koyama K, Miyazaki-J, Sugiyama T, Miura N. Resistance to fulminant hepatitis and carcinogenesis conferred by overexpression of retinoblastoma protein in mouse liver. Hepatology 33: 948-955. 2001.
7. Korinek V, Barker N, Morin PJ, van Wichen D, de Weger R, Kinzer KW, Vogelstein B, Clevers H. Constitutive transcriptional activation by a β-catenin-Tcf complex in APC-/- colon carcinoma. Science 275: 1784-1787. 1997.
8. Yamamoto H, Ihara M, Matsuura Y, Kikuchi A. Sumoylation is involved in β-catenin-dependent activation of Tcf-4. EMBO J 22: 2047-2059. 2003.
9. Sugimura H, Mori H, Nagura K, Kiyose S, Tao H, Isozaki M, Igarashi H, Shinmura K, Hasegawa A, Kitayama Y, Tanioka F. Fluorescence in situ hybridization analysis with a tissue microarray: 'FISH and chips' analysis of pathology archives. Pathol Int 60: 543-550. 2010.

10. Sugimura H. Detection of chromosome changes in pathology archives: an application of microwave- assisted fluorescence in situ hybridization to human carcinogenesis studies. Carcinogenesis 29: 681-687. 2008.
11. Ishimoto T, Nagano O, Yae T, Tamada M, Motohara T, Oshima H, Oshima M, Ikeda T, Asaba R, Yagi H, Masuko T, Shimizu T, Ishikawa T, Kai K, Takahashi E, Imamura Y, Baba Y, Ohmura M, Suemastu M, Baba H, Saya H. CD44 variant regulates redox status in cancer cells by stabilizing the xCT subunit of system xc- and therapy promotes tumor growth. Cancer Cell 19: 387-400. 2011.
12. Calvisi DF, Factor VM, Loi R, Thorgeirsson SS. Activation of β-catenin during hepatocarcino-genesis in transgenic mouse models: Relationship to phenotype and tumor grade. Cancer Res 61: 2085-2091. 2001.
13. Evan GI, Wyllie AH, Gilbert CS, Littlewood TD, Land H, Brooks M, Waters CM, Penn LZ, Hancock DC. Induction of apoptosis in fibroblasts by c-myc protein. Cell 69: 119-128. 1992.
14. Hermeking H, Eick D. Mediation of c-Myc-induced apoptosis by p53. Science 265: 2091-2093. 1994.